Copper Oxide Layers Obtained via Anodization for Electrowetting on Dielectrics

R. Bernasconi*, A. Bellantone, F. Liberale, L. Magagnin

Dipartimento di Chimica, Materiali e Ingegneria Chimica "Giulio Natta", Politecnico di Milano, via Mancinelli 7, 20131, Milano, Italy

* Corresponding author: roberto.bernasconi@polimi.it

Introduction

Electrowetting in a fluid is defined as the change in contact angle, and thus wettability, between the fluid itself and a surface as a result of the application of an electric field [1 - 4]. To observe this phenomenon is fundamental the presence of a dielectric insulating layer on top of a conductive substrate. In the case of water as electrowetting fluid the insulating layer is in general a fluoropolymer, which is able to provide high initial contact angles [3, 4]. A transition from a hydrophobic to a hydrophilic behavior can be observed as a consequence of the application of a difference in potential between the water and the conductive substrate. Electrowetting applications include the realization of displays [5], variable focal lenses [6, 7] and lab-on-chip components [8]. In particular in the last few years the research on electrowetting on flexible substrates [9 - 11] is acquiring a strategic importance for its industrial applications, like the realization of flexible displays.

Electrowetting is described theoretically by the well-known Young-Lippmann equation [1 - 4], which correlate the variation in contact angle to the voltage applied, the thickness of the insulating layer and its dielectric constant. However, even if the phenomenon has already been implemented in the industry [12], some aspects are still not completely understood. These include the two most studied: saturation and hysteresis of the contact angle. The first consists in the reaching of a limit contact angle that cannot be overcome by subsequent increases in potential [13], the latter consists in a decrease in the contact angle variation as a consequence of voltage cycles [4]. Together with these theoretical challenges also some technological problems still need to be addressed. These comprise corrosion of the metallic substrate during usage of the device and poor bonding between the polymer and the metal.

The intercalation of an oxide layer between the polymer and the metal has been proposed as a possible solution to these problems [14]. A suitable oxide can in principle favor the adhesion between the polymer and the substrate and increase the corrosion resistance of the latter. It has been noticed as well that the presence of a high dielectric oxide layer can be beneficial for the final performances [14]. The deposition of the oxide layer on top of the metal can be accomplished choosing appropriately the metal itself and performing anodization. Techniques like CVD, PVD and others are not realistic alternatives due to the high cost. Between the possible substrates, the most immediate choice is valve metals. These materials, which include Al and Ta as examples, are easy to anodize and the resulting oxide layers are characterized by a very good uniformity and compactness together with high dielectric constants (9 for Al_2O_3, 22 for Ta_2O_5, 25 for HfO_2). Electrowetting has already been tested for example on anodized aluminum [15]. However these metals are also difficult to manufacture in thin films or are costly (in particular materials like Ta or Hf).

The aim of the present work is thus to investigate the possibility to use copper (I) oxide as dielectric layer to perform electrowetting. The reason for this is related to some attractive properties of such metal: high conductivity, ease of manufacturing in thin layers by mean of cheap techniques like electrodeposition and the possibility to obtain adherent oxides. Copper (I) oxide was selected despite the lower dielectric constant with respect to copper (II) oxide (7.6 instead of 18.1) because it's easier to obtain in adherent layers. Different anodization processes to obtain Cu_2O are present in the literature [16-18]. A process was thus selected and some parameters like current density, temperature and anodization time were varied to analyze their influence on the final oxide layer. The samples obtained were thus characterized using different techniques. Finally electrowetting was performed on the anodized samples after application of a fluoropolymer. The saturation levels and the hysteresis behavior were investigated.

Experimental methods

The copper used in the experiments is a laminate with a thickness of about 200 μm and purity higher than 99.9 % provided by RS. For the anodization a 2 M NaOH solution was employed. All chemicals were purchased by Sigma Aldrich and used as received. The experimental setup was made up of a 250ml becker containing the solution, two small copper plates to be used as cathode and anode respectively and of a potentiostat-galvanostat Amel 7050 to provide the anodization currents and to register the potential transients during the anodization itself. Current density, temperature and anodization time were varied as indicated in the text. The copper plates were degreased with acetone, washed in deionized water and dried with a nitrogen flux. The solution was slightly agitated with a magnetic stirrer during the process. At the end of each anodization every sample was washed with deionized water and dried with a nitrogen flux. For SEM analysis, a Zeiss Evo 50 EP equipped with an EDS module Oxford Inca Energy 200 EDS was used. GDOES was performed on the samples using a Spectruma Analyser 750, while for XRD a Philips PW 1830 equipped with a vertical goniometer PW 1820 was employed. Laser profilometry was performed by mean of a UBM laser profilometer Microfocus. For the electrowetting tests, a 0.6% solution of AF 1600 fluoropolymer from Dupont in FC40 solvent from 3M was employed. In particular the samples were immersed for 5 seconds inside a beaker containing the solution and then dried in air. After 30 minutes a second

and a third immersions were performed, and after other 30 minutes an annealing at 200°C in air for 1 hour in a Salvislab vacucenter. Using a potentiostat EA-PSI 8360-IST it was possible to supply electrical charges to the drops coming out from a syringe by means of the needle and perform thus saturation and hysteresis tests. The contact angle data were recorded in three points of each sample by mean of a micro camera and a software to analyze the shape of the drop.

Results and discussion

In the first part of the experimentation the anodization of copper was investigated. In particular the influence of operating parameters like current density, temperature and time was studied and correlated to the morphology of the oxide obtained.

Influence of current density on anodization

Anodization current density was varied in the range 2 - 16 mA/cm^2 with 2 mA/cm^2 steps to investigate its influence on the oxide layer, while temperature was kept constant at 90 °C and anodization time at 1 min. In all the cases the surface of copper covered with a black oxide layer. In the case of high anodization currents ($\geq$ 12 mA/cm^2) it was possible to observe the formation of a black powder layer on the surface of the samples. This layer is detrimental for the subsequent application of the fluoropolymer, as the particles can create dishomogeneities in the distribution of the coating. To investigate the nature of the dusty phase formed on the surface the voltage transients during anodization were recorded and compared with the microstructures observed with SEM and the XRD results. Figure 1 reports the results obtained performing chronopotentiometry.

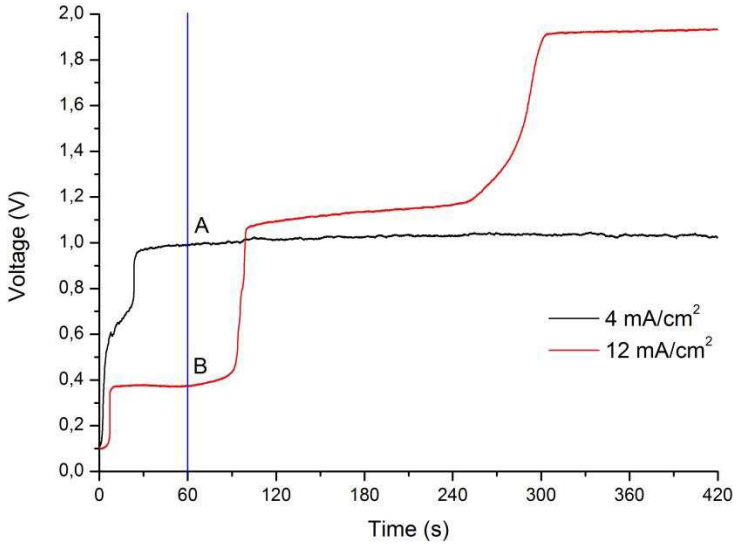

Figure 1. Potential transients for 4 and 12 mA/cm^2 anodization currents; 90 °C

The typical transient for copper anodization in current control presents a first part where the current increases fast and another part characterized by the presence of one or

more steady voltage steps. The first sustained increase in current is connected with the initial covering of the surface with a continuous oxide layer, as confirmed by visual inspection of the sample during the process. In the case of the 4 mA/cm^2 anodization this zone is located between 0 s and 25 s (figure 1), while in the case of the 12 mA/cm^2 anodization it can be individuated between 0 s and 6 s. A first effect of a lower current is thus an increase of the time needed to totally cover the surface with a first uniform layer of oxide. Another effect is on the number of steady voltage steps present in the transient. In the case of the 4 mA/cm^2 anodization only one step can be seen from figure 1, but in the case of the 12 mA/cm^2 anodization three steps can be observed (6 s - 90 s; 90 s - 300 s and 300 s - 420 s). Different potentials at same anodization time imply different grow processes, and each passage from a step to another is connected with a change in the grow conditions of the oxide layer. To exemplify this two samples anodized for 60 s at different currents (4 and 12 mA/cm^2) were analyzed using SEM and XRD, and the results for the first technique are reported in figures 2 and 3.

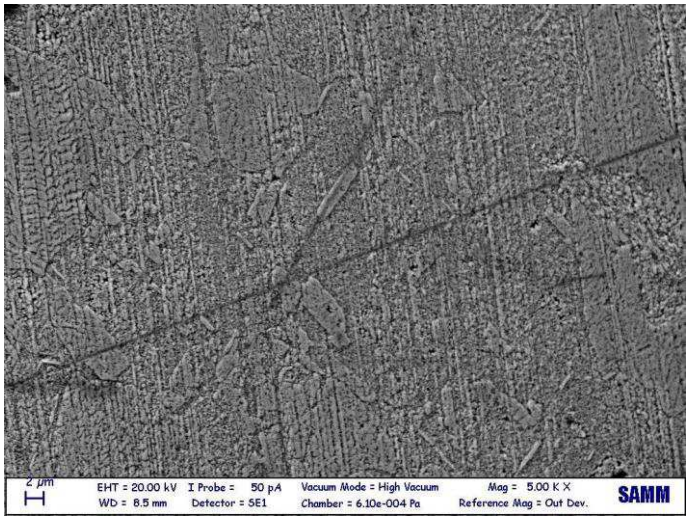

Figure 2. SEM of the sample anodized at 4 mA/cm^2, 90 °C and 60 s

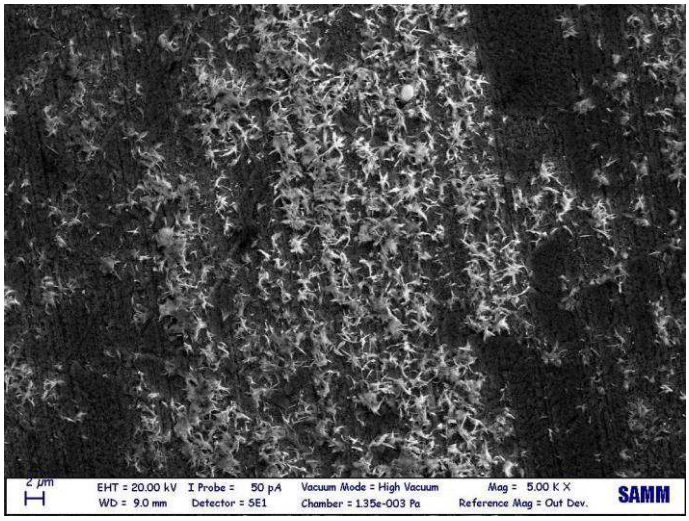

Figure 3. SEM of the sample anodized at 12 mA/cm^2, 90 °C and 60 s

The two samples, obtained in the conditions identified by A and B in figure 1, are characterized by different morphologies. Situation A (4 mA/cm^2) produces an oxide layer compact and adherent to the surface (figure 2), while situation B (12 mA/cm^2) gives a discontinuous coating with a dusty phase on top (as visible in figure 3). Comparing the morphologies with the voltage transients it can be noticed that situation B is characterized by a current density higher than situation A but also by a lower potential. This is a consequence of a lower shielding effect induced by the oxide formed on the surface, which can be related to a more porous and inhomogeneous structure. Such low quality oxide layer is visible in figure 3, where the high grow rate favored the formation of irregular structures on the surface and of a porous oxide layer. On the contrary figure 2 depicts a more homogeneous oxide, growth at higher potentials and lower anodization rates.

Another important effect induced by the higher currents employed can be observed on the phase composition of the oxide. Figure 4 and 5 report the XRD analysis performed for samples A and B.

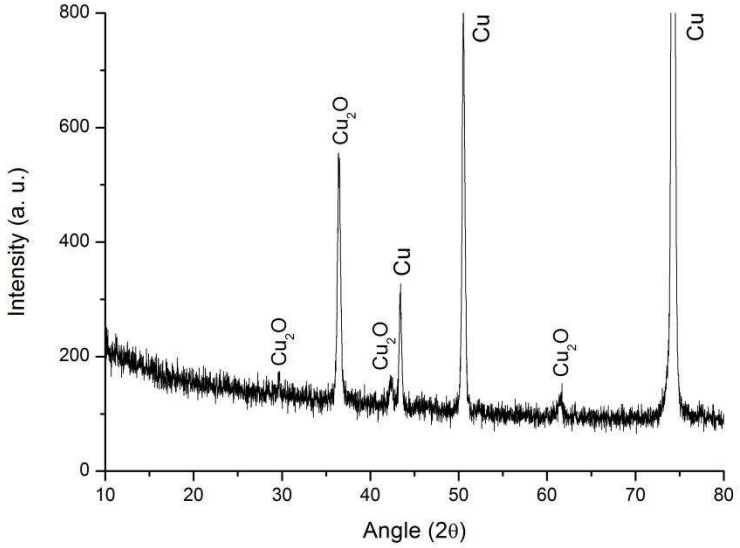

Figure 4. XRD of the sample anodized at 4 mA/cm^2, 90 °C and 60 s

If during anodization a low current (situation A) is used a pure cuprite (Cu_2O) layer can be obtained (figure 4). At high currents (situation B) the formation of tenorite (CuO) along with cuprite was observed (figure 5). The presence of tenorite is negative, since this form of copper oxide presents a different dielectric constant with respect to cuprite.

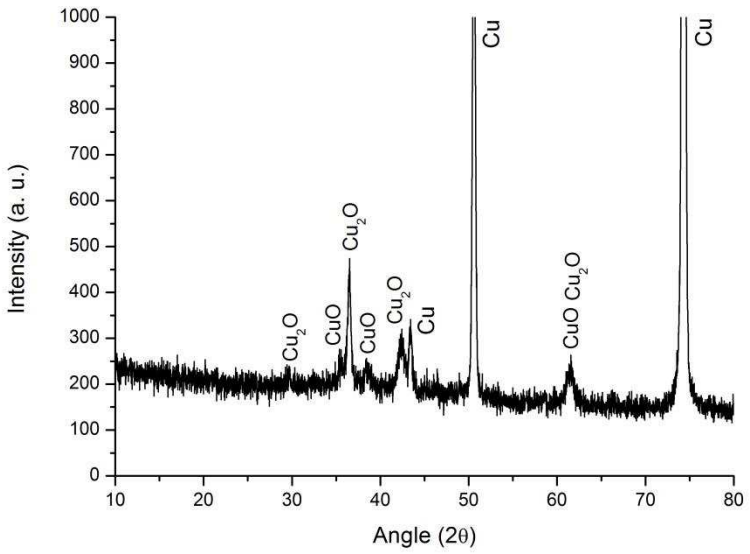

Figure 5. XRD of the sample anodized at 12 mA/cm^2, 90 °C and 60 s

Considering the results disclosed, a low current (4 mA/cm^2) was selected to achieve uniform and adherent oxide layers composed of pure cuprite.

Effect of temperature on anodization

The effect of temperature was investigated changing the anodization conditions. Figure 6 reports the voltage transients obtained at 60 °C as anodization temperature instead of 90 °C (keeping constant the current at 4 mA/cm^2).

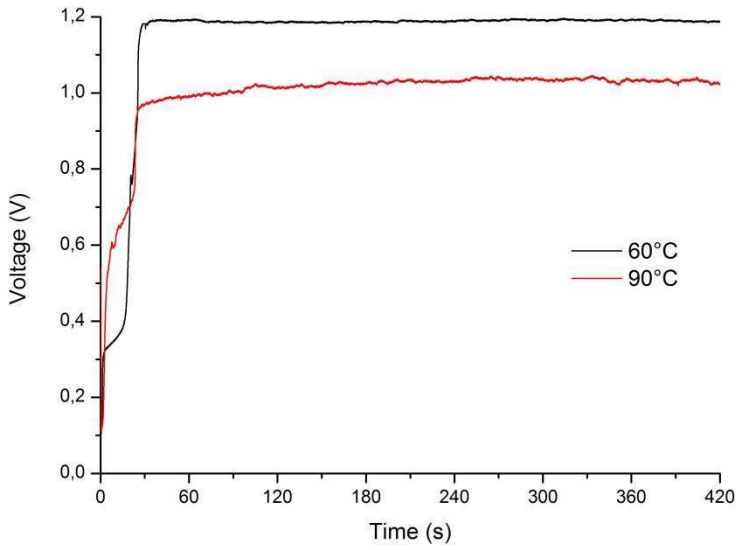

Figure 6. Potential transients for 4 mA/cm^2 anodization current; 90 °C and 60 °C

From figure 6 it's evident that an increase in temperature poorly affects the duration of the initial surface covering step (that is constant at 20 s). The most important effect is the increase in the anodization potential, as a consequence of the decreased conductivity of the electrolyte. No new voltage steps can be observed, making thus possible to predict a morphology similar to the samples obtained at 90 °C. Figure 7 represents the surface of the sample obtained at 60°C, 4 mA/cm^2 for 60 s.

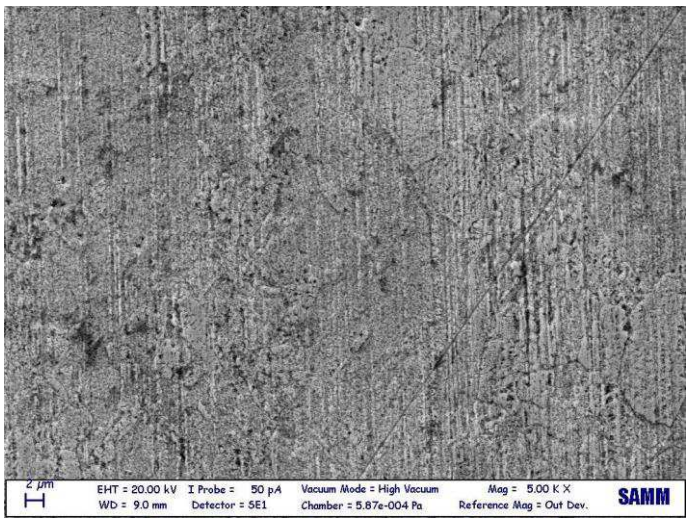

Figure 7. SEM of the sample anodized at 4 mA/cm^2, 60 °C and 60 s

In the image a morphology similar to the one depicted in figure 2 can be observed, as deduced from the shape of the voltage transient in figure 6. The oxide layer obtained was also in this case adherent and compact. XRD showed no secondary phases formation in the 60 °C anodized sample, confirming the presence of pure cuprite.

Influence of time

The influence of anodization time on the oxide layer was studied keeping constant the current density and the temperature at 4 mA/cm^2 and 60 °C respectively. Anodization times between 1 and 7 minutes were then applied and the resulting oxide was characterized with XRD to observe possible phase distribution changes. The results obtained are reported in figure 8.

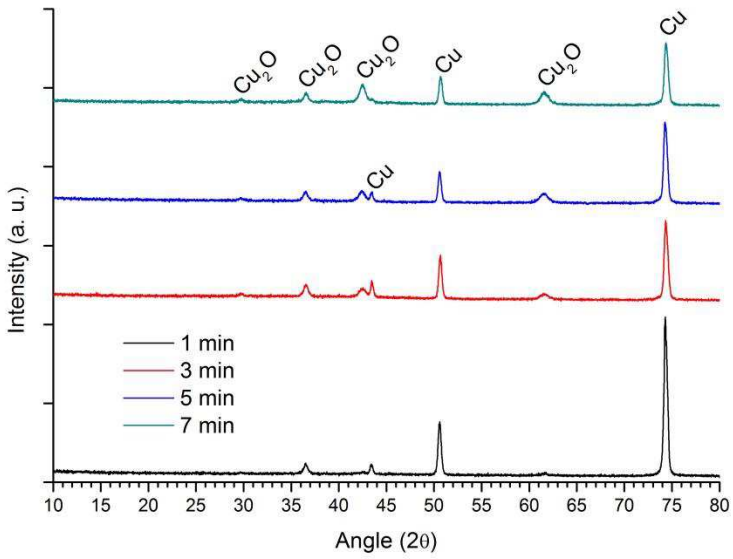

Figure 8. Comparation of the XRD graphs for the samples obtained at increasing anodization times (4 mA/cm^2 and 60 °C)

From the picture it can be immediately noticed that the anodization time increase doesn't introduce new crystallographic phases in the layer. The only effect observed in figure 8 is the increase in thickness of the oxide layer at the expenses of the copper bulk, with the cuprite peaks progressively growing in intensity according to the increasing anodization time. Compact and adherent layers were obtained in all the cases.

To evaluate the thickness of the oxides, GDOES was performed on the samples obtained at different anodization times. Figure 9 represents the Cu signal recorded.

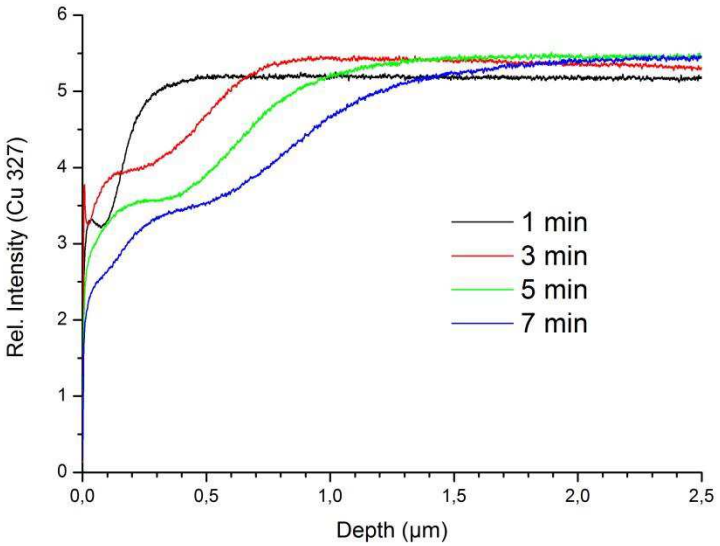

Figure 9. GDOES Cu signal recorded for the samples anodized at different times

From image 9 the thickness of the oxide can be evaluated considering the point where the concavity of each line changes. Figure 10 reports the results obtained together with an exponential fitting (red line).

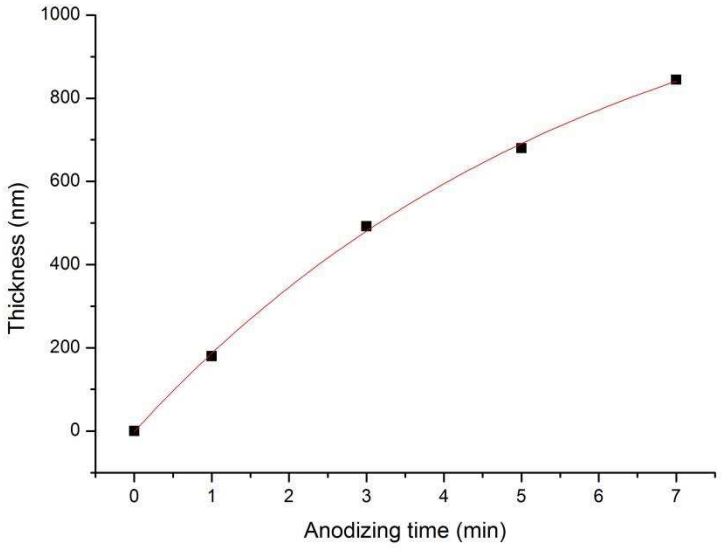

Figure 10. Oxide thickness as a function of the anodizing time (60 °C; 4 mA/cm^2)

Roughness was evaluated as well with a laser profilometer and the results obtained are represented in figure 11.

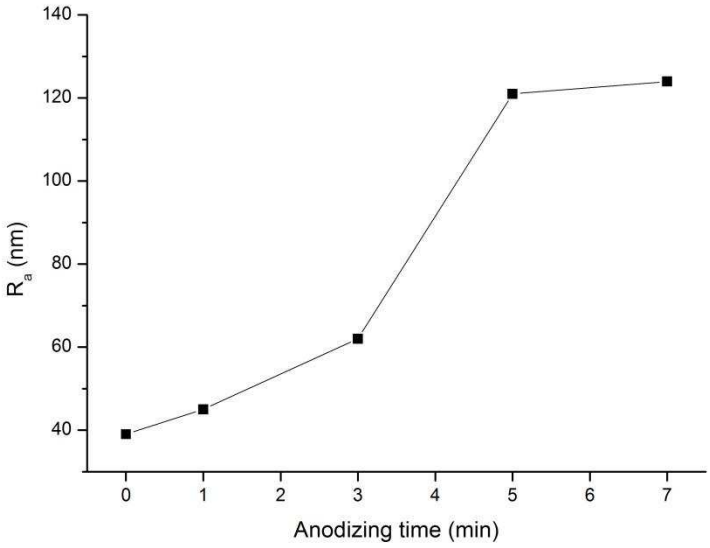

Figure 11. Roughness R_a as a function of the anodization time

A progressive increase of the roughness with the anodization time can be noticed observing the graph. The initial mirror-like appearance of the copper substrate was lost especially in the 5 min and 7 min anodization cases, where a strong increase in R_a was observed.

Electrowetting tests

After the application of AF1600 on the samples, the possibility to achieve electrowetting was investigated. Saturation and hysteresis tests were performed.

Saturation tests. A droplet of water was placed on the surface of the sample and increasing potentials were applied between the electrode placed in the droplet and the copper substrate. To do this samples anodized at 4 mA/cm^2 and 60 °C for different times were employed. The results obtained are represented in figure 12.

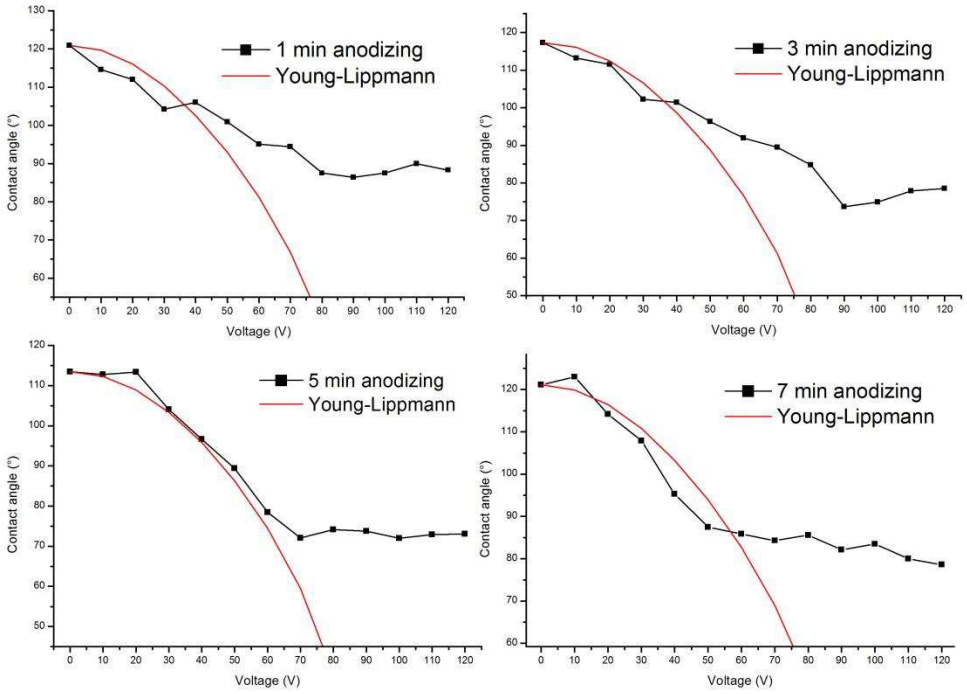

Figure 12. Saturation results for samples anodized at different times superimposed with the corresponding Young-Lippman equations

The results obtained were compared with the theoretical prediction from the Young-Lippman equation (figure 12). In particular the expression of the relationship employed is visible in equation 1.

$$\cos\theta_V = \cos\theta_0 + (\varepsilon_0\varepsilon_r V^2) / (2\delta\gamma_{LG}) \qquad [1]$$

where θ_V is the angle at the potential V, θ_0 is the initial angle at 0 V, ε_r is the dielectric constant of the dielectric layer, δ is the thickness of the dielectric and γ_{LG} is the surface energy between water and its vapor. In this expression the dielectric constant of the oxide/polymer layer was obtained using equation 2.

$$\varepsilon_r = (\varepsilon_{oxide}\delta_{oxide} + \varepsilon_{polymer}\delta_{polymer})/\delta \quad [2]$$

The thickness δ of the dielectric layer is given by equation 3, where the thickness of the oxide δ_{oxide} was obtained from the data in figure 10 and the thickness of the polymer $\delta_{polymer}$ was estimated to be 800 nm from a fitting procedure operated on the experimental data.

$$\delta = \delta_{oxide} + \delta_{polymer} \quad [3]$$

All the samples show electrowetting upon application of a voltage, and the behavior is in good agreement with what predicted by the Young-Lippman equation. Moreover, all the samples present a saturation level, as clearly evident in figure 12. The deviations from the Young-Lippman model can be ascribed to a non-ideal distribution of the polymer on the surface as a consequence of the dip coating method employed to apply AF1600. Such deviations are due to differences in thickness between the samples and not on the same sample (3 tests were performed in different zones of each sample to obtain the data presented). The results obtained are characterized by a good reproducibility over different samples presenting the same processing parameters.

Hysteresis tests. Hysteresis tests were performed by cyclically applying a voltage between the electrode placed in the droplet and the copper substrate to obtain advancing and receding wetting angles. The potential was allowed to change between 0 and 60 V in the first data set and between 0 and 90 V in the second one. Figure 13 reports the data obtained for the 0 - 60 V series and figure 14 for the 0 - 90 V series.

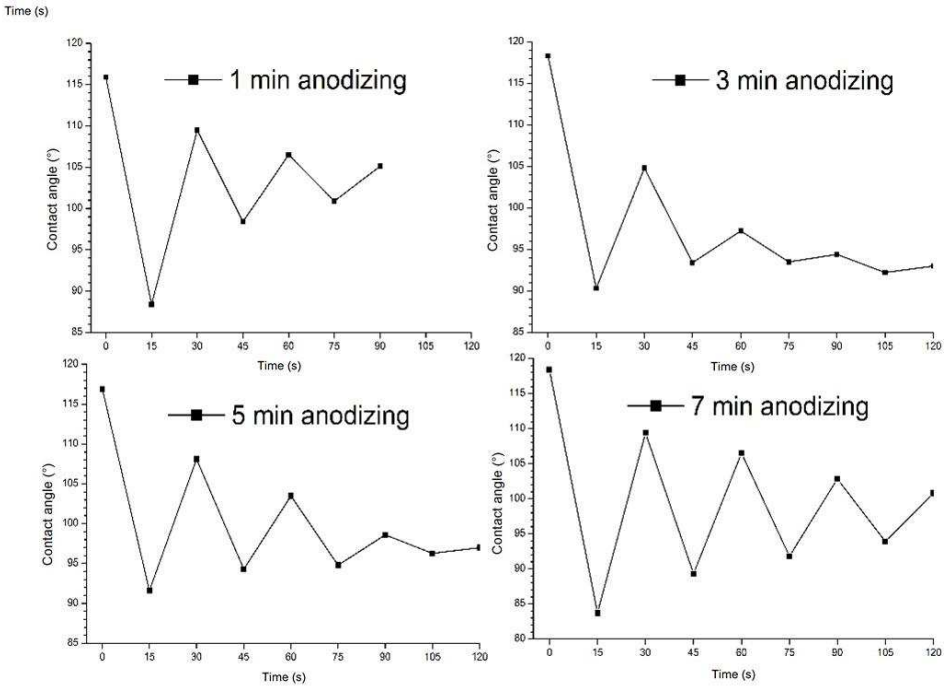

Figure 13. Hysteresis behavior on 4mA/cm^2 anodized samples at 60°C for different times. Potential varied between 0 and 60 V

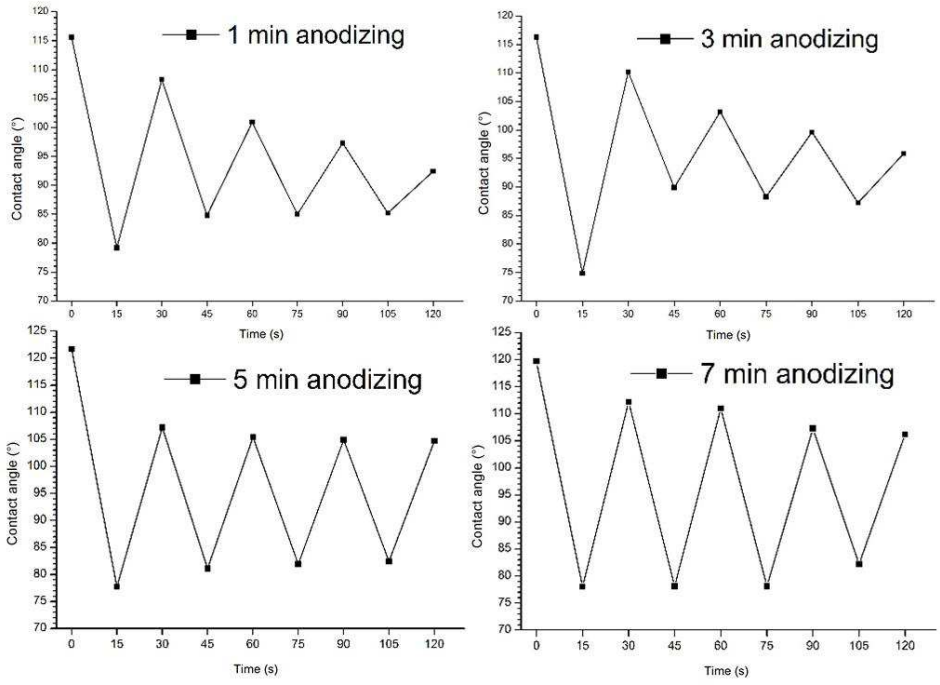

Figure 14. Hysteresis behavior on 4mA/cm^2 anodized samples at 60°C for different times. Potential varied between 0 and 90 V

From the images a general improvement of the electrowetting stability using high anodization times can be observed. Hysteresis is lower when using 90 V instead of 60 V, and this is probably related to the higher energy available to overcome charge trapping in the water droplet. Acceptable stability of the electrowetting phenomenon can be however observed in all the cases at 90 V, with a passage through the wetting/non wetting barrier (for convention at 90°) in all the cases. Also in this case variations between the samples can be attributed to a not constant thickness of the polymer layer as a consequence of the method used for its application.

Conclusions

In the present work electrowetting on copper oxides obtained from anodization was investigated for the first time. The influence of parameters like current density, temperature and anodization time was evaluated. It was noticed that current density plays an important role on the morphology of the oxide film that can be obtained, with compact and continuous films composed of pure cuprite obtained at current densities lower than 12 mA/cm^2. The grow rate of the oxide was found to follow an exponential trend, with thicknesses in the 800 nm range for anodization times up to 7 min. After the application of AF1600, all the samples showed electrowetting. The electrowetting behavior of the samples was found to be in good agreement with the Young-Lippman equation. Hysteresis performance of the samples was characterized by a good behavior for some of the samples and a loss in performance for other samples. This is a consequence of the polymer layer thickness, which is not completely uniform in all the samples. A more stable behavior can however be argued in the case of the thicker oxide layers. The present

work demonstrated the possibility to operate electrowetting on copper oxide layers coated with a fluoropolymer. Moreover, the characterization operated can constitute a reference for the anodization of electrodeposited copper coatings employed as conductive layers in flexible displays technology.

References

1. F. Mugele and J.C. Baret, *J. Phys. Condens. Matter*, **17**, R705 (2005).
2. R. Shamai, D. Andelman, B. Berge and R. Hayes, *Soft Matter*, **4**, 38 (2008).
3. C. Quilliet and B. Berge, *Curr. Opin. Colloid Interface Sci.*, **6**, 34 (2001).
4. Y.P. Zhao and Y. Wang, *Rev. Adhes. Adhesives*, **1**, 114 (2013).
5. Y. Lao, Ultra-high transmission electrowetting displays. Master thesis, University of Cincinnati: Cincinnati (2008).
6. S. Kuiper and B.H.W. Hendriks, *Appl. Phys. Lett.*, **85**, 1128 (2004).
7. C. Li and H. Jiang, *Appl. Phys. Lett.*, **100**, 231105 (2012).
8. M.G. Pollack, A.D. Shenderov and R.B. Fair, *Lab Chip*, **2**, 96 (2002).
9. A.J. Steckl, H. You and D.Y. Kim, In: Flexible electrowetting and electrowetting on flexible substrates, Proceedings of SPIE 2011, San Francisco, CA, USA, January 22, 2011, vol. 7956 795907.
10. H. You and A.J. Steckl, *J. Adhesion Sci. Technol.*, DOI: 10.1163 / 156856111X600244 (2011).
11. K. Zhou, K.A. Dean and J. Heikenfeld, Flexible Electrofluidic Displays Using Brilliantly Colored Pigments. SID Symp. Dig. Tech. (2010) 484-486.
12. www.liquavista.com, last access 24th October 2015
13. D. Klarman, D. Andelman and M.A. Urbakh, *Langmuir*, **27**, 6031 (2011).
14. M. Mibus, X. Hu, C. Knospe, M.L. Reed and G Zangari, *Curr. Nanosci.*, **11**, 333 (2015).
15. F. Liberale, R. Bernasconi and L. Magagnin, *Curr. Nanosci.*, **11**, 286 (2015).
16. F. Caballero-Briones, A. Palacios-Padrós, O. Calzadilla and F. Sanz, *Electrochim. Acta*, **55**, 4353 (2010).
17. N.K. Allam and C.A. Grimes, *Mater. Lett.*, **65**, 1949 (2011).
18. L.A. Svetlichnaya, L.P. Mileshko, and A.N. Korolev, *Inorg. Mat.*, **44**, 713 (2008).